Effects of nicotine on the metabolism and gene expression profile of Sprague-Dawley rat primary osteoblasts

DAN LIANG[1*], KE-JING WANG[1,2*], ZHI-QUN TANG[1], RUN-HE LIU[1], FULEI ZENG[1], MIAO-YING CHENG[1], QI-SI LIAN[1] and HONG-KUN WU[1]

[1]State Key Laboratory of Oral Diseases, National Clinical Research Center for Oral Diseases, West China Hospital of Stomatology, Sichuan University, Chengdu, Sichuan 610041; [2]State Key Laboratory of Military Stomatology and National Clinical Research Center for Oral Diseases and Shaanxi Key Laboratory of Oral Diseases, Department of Operative Dentistry and Endodontics, School of Stomatology, The Fourth Military Medical University, Xi'an, Shaanxi 710032, P.R. China

Received September 25, 2017; Accepted March 5, 2018

DOI: 10.3892/mmr.2018.8884

Abstract. Smoking is a risk factor associated with bone and oral diseases, particularly periodontitis. Nicotine, the major toxic component of tobacco, is able to affect the quality and quantity of bone. Osteoblasts serve an important role in bone formation. Thus far, the effects of nicotine on metabolism-associated gene and protein expression in osteoblasts have been controversial and the mechanisms remain unclear. The present study assessed alterations in osteogenic activity by performing a Cell Counting kit-8 assay to investigate proliferation, Annexin V-fluorescein isothiocyanate/propidium iodide staining to investigate apoptosis, alizarin red staining to investigate the formation of mineralized nodules, reverse transcription-quantitative polymerase chain reaction and western blotting to investigate the mRNA and protein levels of collagen I, alkaline phosphatase, bone osteocalcin, bone sialoprotein and osteopontin; and mRNA microarray expression analysis, Kyoto Encyclopedia of Genes and Genomes and Gene Ontology analysis to investigate the whole genome expression profile of Sprague-Dawley (SD) rat primary osteoblasts following treatment with different concentrations of nicotine. The results demonstrated that nicotine inhibited proliferation, promoted early apoptosis and inhibited mineralized nodule formation in a dose-dependent manner by regulating alkaline phosphatase activity and the expression of osteoblast metabolism-associated genes and proteins. According to microarray analysis, several genes associated with bone metabolism and genes in the Hedgehog and Notch signaling pathways were downregulated significantly in nicotine-treated osteoblasts. The results of the present study indicated that nicotine may serve an inhibitory, dose-dependent role in SD rat primary osteoblasts that may be caused by the perturbation of genes and signaling pathways associated with bone formation. These results may provide a theoretical basis for future research regarding bone metabolism and targeted treatment of oral diseases associated with smoking.

Correspondence to: Professor Hong-Kun Wu, State Key Laboratory of Oral Diseases, National Clinical Research Center for Oral Diseases, West China Hospital of Stomatology, Sichuan University, 14 Third Section of Renmin South Road, Chengdu, Sichuan 610041, P.R. China
E-mail: 415402020@qq.com

*Contributed equally

Key words: nicotine, Sprague-Dawley rat osteoblasts, osteogenic activity, gene expression profile

Introduction

Smoking is a strong risk factor for various oral diseases and particularly for periodontitis (1,2), which primarily presents as alveolar bone resorption. A higher prevalence and more severe form of periodontitis has been associated with smokers compared with non-smokers (3). Nicotine is the major toxic component of tobacco and regulates bone metabolism by accelerating the loss of periodontal tissue attachment and alveolar bone absorption, exacerbating periapical disease, inducing peri-implantitis and decreasing the rate of bone regeneration following tooth extraction or surgery (4-7). The inhalation of tobacco leads to the accumulation of toxic components in the circulatory system and local oral tissue (8). Our unpublished data indicated that nicotine is directly deposited on tooth surfaces and in alveolar bone; therefore, we inferred that the deposition of nicotine may serve an important role in regulating bone metabolism.

Bone metabolism depends on the dynamic balance between bone formation and absorption. Osteoblasts have an important role in bone formation. En-Nosse *et al* (9) identified a number of types of nicotinic acetylcholine receptors, to which nicotine can specifically bind, on the surface of osteoblasts. Therefore, the effects of nicotine on alveolar bone may be partially due to its effects on osteoblasts. In an *in vitro* osteogenesis process, osteoblasts adhere to the bone defect zone, synthesize and secrete collagen I to form bone matrix, and subsequently secrete various non-collagen matrix proteins, including

alkaline phosphatase (ALP), bone osteocalcin (OCN), bone sialoprotein (BSP) and osteopontin (OPN) (10), which serve important roles in the mineralization of bone matrix.

Previous studies have indicated the effects of nicotine on the proliferation and differentiation of osteoblasts in different types of models (11-15). Few of the studies used primary osteoblasts. Additionally, the results remain controversial, and the underlying mechanisms unclear. A number of the studies have demonstrated that nicotine has an inhibitory effect on bone metabolism, while others demonstrated a biphasic effect. In the present study, primary Sprague-Dawley (SD) rat osteoblasts were cultured and the effects of different concentrations of nicotine on osteogenic activity and the whole genome expression profile were investigated to clarify the molecular mechanisms and to provide a theoretical basis for diseases caused by smoking and associated with the imbalance of bone metabolism.

Materials and methods

Cell culture. The current study was approved by the Ethics Committee of West China Hospital of Stomatology of Sichuan University (Chengdu, China). A total of 80 male newborn SD rats (<72 h old, 6-8 g) were obtained from the West China Animal Experiment Center of Sichuan University and bred in constant specific-pathogen-free conditions (relative humidity, 50%; temperature, 25˚C; 12-h light/dark cycle) and had free access to breast milk. The newborn rats were sacrificed by cervical dislocation. Primary osteoblasts were obtained from the parietal bone; the bone was chopped into 1 mm^2 fragments, rinsed with PBS (Hyclone; GE Healthcare Life Sciences; Logan, UT, USA), digested with 5 ml trypsin (0.25%; Sigma-Aldrich; Merck KGaA, Darmstadt, Germany) for 10 min at 37˚C and incubated with 10 ml collagenase I (1 g/l; Sigma-Aldrich; Merck KGaA) at 37˚C for 90 min. The fragments were seeded into 25-cm^2 flasks at a density of 15 fragments per flask, mixed with Dulbecco's modified Eagle's medium (DMEM; Hyclone; GE Healthcare Life Sciences) containing 10% fetal bovine serum (Hyclone; GE Healthcare Life Sciences), 100 units/ml penicillin and 100 μg/ml streptomycin (Sigma-Aldrich; Merck KGaA) and then cultured at 37˚C with 5% CO_2. The medium was changed every other day. Osteoblasts from passages 2-4 were used in subsequent experiments.

Cell identification. Cells were cultured at 37˚C with 5% CO_2 in osteogenic induction medium containing DMEM with 10% fetal bovine serum, β-glycerophosphate (10 mmol/l) and L-ascorbate (50 μg/ml), all purchased from Sigma-Aldrich (Merck KGaA), in 6-well plates at a density of $5x10^4$ cells/ml. When the cells reached 80% confluence, they were thrice rinsed with PBS and fixed with 95% ethanol for 10 min at the room temperature. ALP was stained with a BCIP/NBT kit (Beyotime Institute of Biotechnology, Haimen, China) and then observed using an inverted microscope (magnification, x200). Following culture for 3 weeks, cells were fixed with 4% polyoxymethylene for 30 min at the room temperature, stained using alizarin red was performed at 37˚C (Cyagen Biosciences Guangzhou, Inc., Guangzhou, China) and observed by an inverted microscope (magnification, x40) to characterize the osteoblasts.

Cell viability and apoptosis. Osteoblasts cultured in 96-well plates at 37˚C with 5% CO_2 at a density of $5x10^4$ cells/ml were exposed to nicotine (Sigma-Aldrich; Merck KGaA) at various concentrations (0, $1x10^{-6}$, $1x10^{-5}$, $1x10^{-4}$ and $1x10^{-3}$ mol/l) for 1, 3, 5 and 7 days. Cell proliferation was evaluated using a Cell Counting kit-8 (CCK-8) kit (Dojindo Molecular Technologies, Inc., Kumamoto, Japan) in accordance with the manufacturer's protocols. The optical absorbance of samples was measured using a microplate reader at a wavelength of 450 nm. Following the culturing of cells ($5x10^4$ cells/ml) with nicotine-containing medium in 25 cm^2 flasks at 37˚C with 5% CO_2 for 7 days, apoptosis was evaluated using an Annexin V-Fluorescein Isothiocyanate (FITC)/Propidium Iodide (PI) Apoptosis Detection kit (Dojindo Molecular Technologies, Inc.), in accordance with the manufacturer's protocols, and detection was performed on a flow cytometer (Beckman Coulter, Inc., Brea, CA, USA). CytExpert software (version 1.0.135.1; Beckman Coulter, Inc.) was used for analysis. The results were interpreted as follows: Active cells [Annexin V-FITC(-)/PI(-)], early-phase apoptotic cells [Annexin V-FITC(+)/PI(-)], and necrotic and late-phase apoptotic cells [Annexin V-FITC(+)/PI(+)].

ALP activity assay. Osteoblasts were cultured in 12-well plates at a density of $5x10^4$ cells/ml at 37˚C with 5% CO_2. When cells reached 70-80% confluence, nicotine-containing medium was added at 0, $1x10^{-6}$, $1x10^{-5}$, $1x10^{-4}$ and $1x10^{-3}$ mol/l concentrations. ALP activity was evaluated after days 4, 7 and 10 using an ALP test kit (Nanjing Jiancheng Bioengineering Institute, Nanjing, China) according to the manufacturer's protocol. The optical absorbance was measured by a microplate reader at a wavelength of 520 nm. The protein concentrations of samples were determined by a BCA kit (Beyotime Institute of Biotechnology) according to the manufacturer's protocol. ALP levels were normalized to the total protein content at the end of the experiment.

Alizarin red staining and quantitative analysis. Osteoblasts were plated in 6-well plates at a density of $5x10^4$ cells/ml. Following incubation with nicotine-containing medium (0, $1x10^{-6}$, $1x10^{-5}$, $1x10^{-4}$ and $1x10^{-3}$ mol/l) at 37˚C with 5% CO_2 for 21 days, 4% paraformaldehyde (Shanghai Chemical Reagent Co., Ltd., Shanghai, China) and 0.1% alizarin red staining solution (Cyagen Biosciences Guangzhou, Inc.) were consecutively added with room temperature incubations of 30 and 5 min, respectively. A digital camera (D610; Nikon Corporation, Tokyo, Japan) was used to capture images. Subsequently, 1 ml PBS and 1 ml OF 10% cetylpyridinium chloride (Sigma-Aldrich; Merck KGaA) were successively added to each well and incubated at 37˚C for 15 min. The optical absorbance of samples was measured using a microplate reader at a wavelength of 562 nm.

Reverse transcription-quantitative polymerase chain reaction (RT-qPCR). Osteoblasts were plated in 6-well plates at a density of $5x10^4$ cells/ml. Following incubation with nicotine-containing medium (0, $1x10^{-6}$, $1x10^{-5}$, $1x10^{-4}$ and $1x10^{-3}$ mol/l) at 37˚C with 5% CO_2 for 7 days, the total RNA was extracted using TRIzol (Invitrogen; Thermo Fisher Scientific, Inc., Waltham, MA, USA). Following quality confirmation of the extracted RNAs, cDNAs were synthesized using

Table I. Primer sequences for reverse transcription-quantitative polymerase chain reaction.

Gene	Sequence		Product size (bp)
	Forward	Reverse	
ALP	CATCATGTTCCTGGGAGATG	GGTGTTGTACGTCTTGGAGA	148
Col1-α1	GTGCTAAGGGTGAAGCTGGT	CATCAGCACCAGGGTTTCCAG	126
OCN	CCTCTCTGACCTGGCAGGT	GGCTCCAAGTCCATTGTTGA	124
OPN	CACTCAGATGCTGTAGCCACTT	GTTGCTTGGAAGAGTTTCTTGCT	126
BSP	CTGAAGAAAACGGGGTCTTTAAG	GAACTATCGCCATCTCCATT	136
Notch1	TCAGCGGGATCCACTGTGAG	ACACAGGCAGGTGAAGTTG	175
Fgf21	AGATCAGGGAGGATGGAACA	TCAAAGTGAGGCGATCCATA	126
β-actin	GAAGATCAAGATCATTGCTCCT	TACTCCTGCTTGCTGATCCACA	111

ALP, alkaline phosphatase; Col1-α1, collagen type I α1; OCN, osteocalcin; BSP, bone sialoprotein; OPN, osteopontin; Fgf21, fibroblast growth factor 21.

a Revert Aid™ First Strand cDNA Synthesis kit (Fermentas; Thermo Fisher Scientific, Inc., Pittsburgh, PA, USA) for 10 min at 20˚C, for 60 min at 42˚C and 10 min at 70˚C. The primers used for the amplification are given in Table I. qPCR was conducted with SYBR® Premix Ex Taq™ II (Tli RNaseH Plus) kit (Takara Biotechnology Co., Ltd., Dalian, China). The reaction mixture (30 μl) contained 3 μl buffer (Mg^{2+} free, 10X), 3 μl $MgCl_2$ (25 mM), 0.36 μl dNTP (25 mM), 1 μl each of 10 μM forward and reverse primers, 1 μl SYBR-Green I (10X), 0.3 μl Taq enzyme (5 U/μl), 5 μl cDNA and 15.34 μl ddH_2O. Amplification was performed using a real-time PCR detection system (Funglyn Biotech, Inc., Richmond Hill, Canada) with temperature cycles set as follows: 94˚C for 2 min, 45 cycles of 94˚C for 20 sec and 56˚C [for ALP, collagen type I α1 (Col1-α1), OCN and OPN], 52˚C (for BSP) or 54˚C (for β-actin) for 20 sec; and 72˚C for 30 sec. Following normalizing the mean quantification cycle (Cq) values, the changes in the expression of ALP, Col1-α1, OCN, OPN and BSP genes were evaluated relative to the expression of β-actin as an internal control gene using the $2^{-\Delta\Delta Cq}$ method, as previously described (16).

Western blot analysis. Cells were incubated with nicotine-containing medium (0, $1x10^{-6}$, $1x10^{-5}$, $1x10^{-4}$ and $1x10^{-3}$ mol/l) for 7 days and then lysed on ice for 30 min using 150 μl radioimmunoprecipitation buffer (Cell Signaling Technology, Inc., Danvers, MA, USA) to extract the protein. Protein concentrations were measured using a BCA kit. Protein samples (50 μg/lane) were subjected to SDS-PAGE on 12% polyacrylamide gels. Gels were run at 80 V for 20 min and 120 V for 50 min. Gel-separated proteins were transferred onto polyvinylidene difluoride membranes at 100 V for 90 min. The transfer membrane was blocked with PBS-0.1% Tween-20 containing 5% bovine serum albumin (Cell Signaling Technology, Inc.) at 4˚C overnight. Following incubation at 4˚C overnight with rabbit or mouse polyclonal IgG antibodies against ALP (cat. no. 11187-1-AP; 1:300), Col1-α1 (cat. no. 14695-1-AP; 1:300), OPN (cat. no. 25715-1-AP; 1:300), β-actin (cat. no. 66009-1-Ig; 1:5,000; all Wuhan Sanying Biotechnology, Wuhan, China), OCN (cat. no. ab13420; 1:300) or BSP (cat. no. ab52128; 1:300; both Abcam, Cambridge, MA, USA), the membranes were incubated at 37˚C for 1 h with biotin-conjugated goat anti-rabbit IgG (cat. no. SA00004-2; 1:20,000; Wuhan Sanying Biotechnology) and biotin-conjugated goat anti-mouse IgG (cat. no. SA00004-1; 1:20,000; Wuhan Sanying Biotechnology). Immunoreactive proteins were visualized using a DAB color reagent kit (OriGene Technologies, Inc., Beijing, China) in the dark. Following image acquisition, the protein bands were quantitatively analyzed by Quantity One analysis software (version 4.6.6; Bio-Rad Laboratories, Inc., Hercules, CA, USA) and the relative expression levels of target proteins were calculated according to the ratio of gray value of target proteins to the gray value of the internal reference protein, β actin.

mRNA microarray analysis. To reveal the differentially expressed gene profiles following nicotine treatment, cells ($5x10^4$ cells/ml) were cultured with nicotine-containing medium ($1x10^{-3}$ mol/l) and medium alone in 25 cm^2 flasks at 37˚C with an atmosphere of 5% CO_2 for 7 days. Following this, osteoblast samples were subjected to whole genome microarray analysis using an Agilent Whole Rat Genome Oligonucleotide Microarray (Agilent Technologies, Inc., Santa Clara, CA, USA). The entire analysis procedure was performed by KangChen Bio-tech, Inc. (Shanghai, China). Using a 2.0-fold cutoff and $P<0.05$ for mRNA expression upregulation or downregulation, the key genes associated with nicotine treatment were identified. The results of microarray analysis were validated by RT-qPCR to detect the expression of Notch1 and Fgf21, which demonstrated significant down- and upregulation, respectively, by microarray analysis. The primers used for amplification are given in Table I. Amplification was performed with annealing and extension at 56˚C for Notch1 and Fgf21 and 54˚C for β-actin. Gene expression was calculated as described above for RT-qPCR.

Kyoto Encyclopedia of Genes and Genomes (KEGG) pathway and Gene Ontology (GO) enrichment analysis. To further investigate the functions of the differentially expressed genes, GO terms were analyzed using the GO database (17)

(http://www.geneontology.org/) and P-values for all genes were calculated in all GO categories, including Cellular Component, Molecular Function and Biological Process terms. The threshold of significance was defined as P<0.05. The data on signaling pathways were obtained from the KEGG pathway database (18) (http://www.kegg.jp/kegg/kegg2.html), and the threshold of significance was defined as P<0.05.

Statistical analysis. All experiments were performed at least in triplicate (n=3 independent experiments). Data are presented as the mean ± standard deviation. The data were analyzed by SPSS software version 16.0 (SPSS, Inc., Chicago, IL, USA). The differences between groups were analyzed by one-way analysis of variance and Student-Newman-Keuls tests. P<0.05 was considered to indicate a statistically significant difference.

Results

Cell identification. Cultured osteoblasts were stained using the BCIP/NBT ALP staining kit and observed on an inverted microscope. A large number of positively stained cells with blue-violet cell membranes and cytoplasmic granules were observed (Fig. 1A). Alizarin red-stained calcified nodules appeared red (Fig. 1B). This result confirmed that the cultured cells were in fact osteoblasts.

Effects of nicotine on early apoptosis. The results of Annexin V-FITC/PI double staining was performed to investigate the early apoptosis of osteoblasts. Quadrant 1 was considered to indicate early apoptotic cells and thus was used for the quantification of apoptosis rates. The results indicated that the early apoptosis of osteoblasts was only significantly promoted by treatment with nicotine concentrations of $1x10^{-4}$ and $1x10^{-3}$ mol/l, compared with the control group (Fig. 2). These results suggested that nicotine promoted the early apoptosis of osteoblasts in a dose-dependent manner.

Effects of nicotine on osteoblast proliferation and ALP activity. As demonstrated in Fig. 3A, compared with the control group, the proliferation of osteoblasts was significantly decreased in all nicotine groups (P<0.05) after 1 and 5 days, whereas proliferation was decreased only in the $1x10^{-3}$-mol/l group after 3 and 7 days (P<0.05). The inhibition of osteoblast proliferation was enhanced by increased nicotine concentrations. Compared with the control group, the ALP activity of all groups was significantly higher compared with the control group on the 4th day (P<0.05; Fig. 3B). On the 7th day, the ALP activity of the cells in all experimental groups was significantly lower compared with the control group (P<0.05; Fig. 3B). However, on the 10th day, only the ALP activity of the $1x10^{-4}$ and $1x10^{-3}$ mol/l groups was significantly lower compared with the control group (P<0.05; Fig. 3B). This suggested demonstrated that nicotine inhibited the proliferation of osteoblasts and ALP activity in a dose-dependent manner.

Effects of nicotine on the mineralized nodule formation of osteoblasts. The results of alizarin red staining revealed decreased numbers of mineralized nodules following treatment with nicotine in a dose-dependent manner (Fig. 3C). Quantification of alizarin red staining demonstrated that the number of mineralized nodules stained in the experimental groups decreased significantly compared with the control group as the nicotine concentration increased (Fig. 3D). These results demonstrated that nicotine suppressed the bone formation of osteoblasts in a dose-dependent manner.

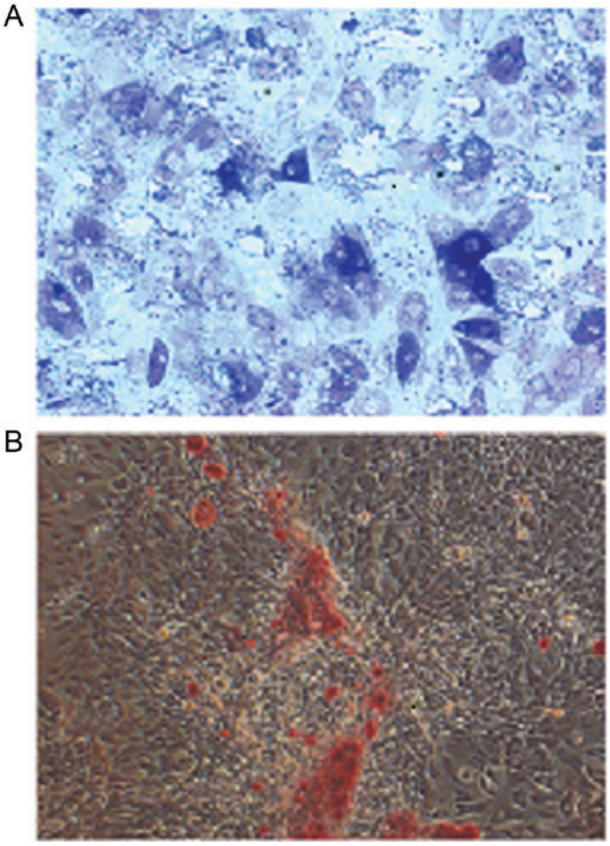

Figure 1. Characterization of Sprague-Dawley rat osteoblasts. (A) Alkaline phosphatase staining demonstrated positive cells with blue-violet cell membranes and cytoplasmic granules (magnification, x200). (B) Alizarin red-stained calcified nodules were stained red (magnification, x40).

Effects of nicotine on osteoblast metabolism-associated mRNA expression. The effect of nicotine on the mRNA expression of genes associated with osteoblast metabolism was investigated by RT-qPCR (Fig. 4). As demonstrated in Fig. 4A, nicotine exhibited no significant effect on the gene expression of ALP in the osteoblasts of SD rats. In addition, there were no significant differences in the expression of Col1-α1 and OCN genes among the control group and the $1x10^{-6}$, $1x10^{-5}$ and $1x10^{-4}$ mol/l groups; however, in the $1x10^{-3}$ mol/l group, the expression level of Col1-α1 and OCN were significantly lower compared with the control group (P<0.05; Fig. 4B and C). The expression of the BSP gene in each experimental group was significantly lower compared with the control group (P<0.05; Fig. 4D). Furthermore, although no significant differences in OPN expression were observed between the control and the $1x10^{-6}$, $1x10^{-5}$ and $1x10^{-4}$ mol/l groups, OPN expression was significantly higher compared with the control group in the $1x10^{-3}$ mol/l group (Fig. 4E). The results suggested that the inhibitory effect of nicotine on bone formation was regulated by the upregulation of OPN mRNA as well as the downregulation of Col1-α1, BSP and OCN mRNA in osteoblasts.

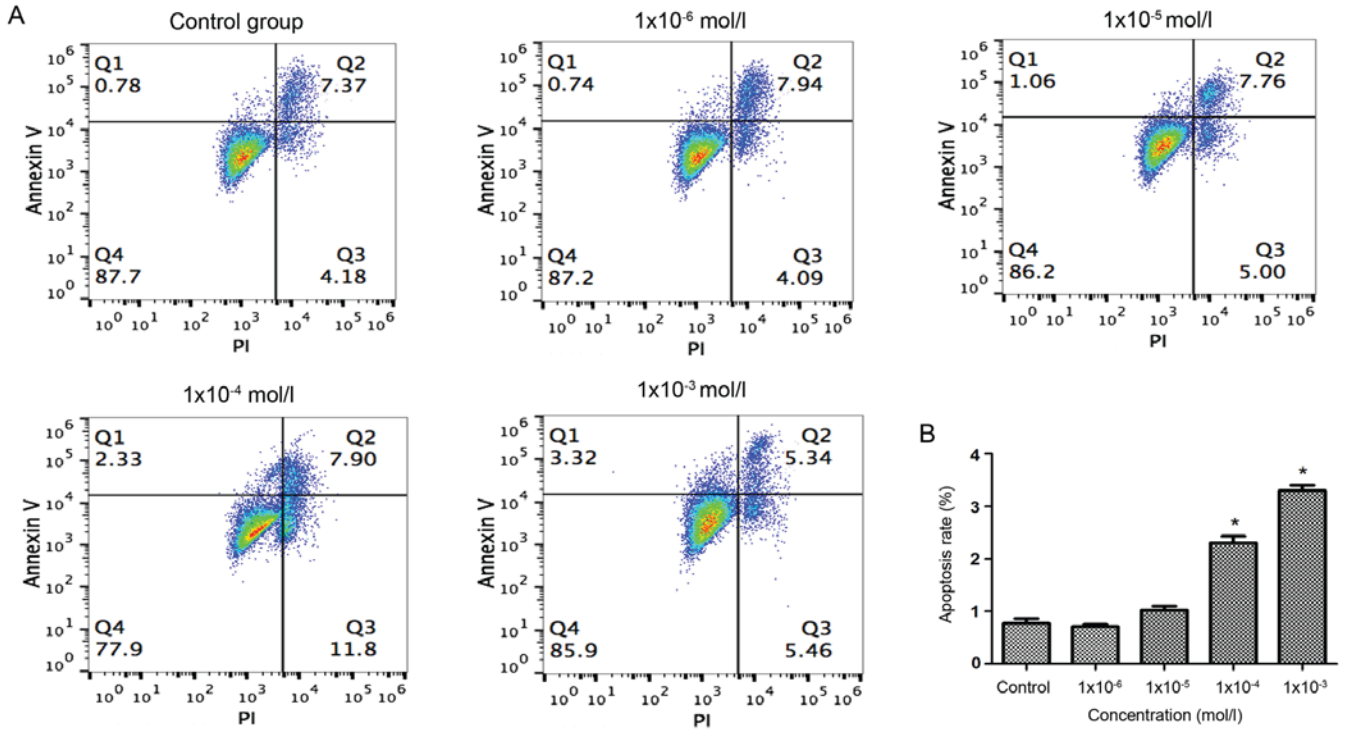

Figure 2. Effects of nicotine on Sprague-Dawley rat osteoblast apoptosis. (A) Representative scatter plots for the apoptosis of control and nicotine-treated osteoblasts following flow cytometry. (B) Quantified results for apoptosis (quadrant 1) demonstrated that, compared with the control group, the early apoptosis of cells was significantly promoted by nicotine at concentrations of $1x10^{-4}$ and $1x10^{-3}$ mol/l after 7 days. Each bar represents the mean ± standard deviation (n=3) *P<0.05 vs. control group. FITC, fluorescein isothiocyanate; PI, propidium iodide.

Effects of nicotine on osteoblast metabolism-associated protein expression. As demonstrated in Fig. 5, the ALP and BSP protein levels were significantly decreased in the $1x10^{-5}$, $1x10^{-4}$ and $1x10^{-3}$ mol/l groups compared with the control group (P<0.05), the expression levels of Col1-α1 and OCN protein in the $1x10^{-4}$ and $1x10^{-3}$ mol/l groups were significantly lower compared with the control group (P<0.05) and the OPN protein level was significantly higher compared with the control group at $1x10^{-4}$ and $1x10^{-3}$ mol/l nicotine (P<0.05). The results indicated that the inhibitory effect of nicotine on bone formation was regulated by the upregulation of OPN protein levels as well as the downregulation of ALP, BSP, Col1-α1 and OCN protein levels in osteoblasts.

Effects of nicotine on the whole genome expression profile of SD rat osteoblasts. Microarray analysis revealed 277 genes with at least 2-fold altered expression and P<0.05 following nicotine treatment, including 121 upregulated genes and 156 downregulated genes. The top 10 upregulated and downregulated genes are presented in Tables II and III, respectively. As demonstrated in Table IV, the expression of genes associated with bone metabolism, including matrix metallopeptidase 3, SMAD family member 3 and latent transforming growth factor b-binding protein 2, were significantly altered. In order to further verify the microarray results, the upregulated and downregulated genes with greatest fold changes were chosen and further analyzed using RT-qPCR. The results demonstrated that the expression of Notch1 was downregulated 5.67-fold and that Fgf21 expression was upregulated 5.94-fold in the osteoblasts of SD rats treated with $1x10^{-3}$ mol/l nicotine compared with the control group, which was consistent with the microarray results (Fig. 6A). Gene Ontology analysis indicated that $1x10^{-3}$ mol/l nicotine altered several functions of the osteoblasts of SD rats in the three main aspects of Cellular Component, Molecular Function and Biological Process. The differentially expressed genes associated with various functions are presented in Fig. 6B. Pathway analysis indicated that differentially expressed genes were primarily associated with signal transduction pathways. The top 10 up and downregulated pathways are presented in Tables V and VI. Among the pathways identified, the Hedgehog and Notch pathways have been previously revealed to directly regulate osteoblast differentiation (19-21). The upregulated and downregulated genes associated with the Hedgehog and Notch pathways are presented in Table VII. These results revealed the potential underlying mechanisms associated with the effect induced by nicotine on the osteogenic activity of osteoblasts.

Discussion

A substantial amount of clinical and experimental research has demonstrated that tobacco smoking has deleterious effects on numerous biological systems, including an association with oral diseases (1). As the major toxic component, nicotine appears to serve a major role in the negative effects of tobacco smoke on bone metabolism, primarily by causing the absorption of alveolar bone. Various studies have investigated the effects of nicotine on the osteogenic activity by analyzing proliferation, differentiation, and specific protein and gene expression. However, the results remain controversial. Fang *et al* (22) reported that nicotine suppressed cellular proliferation and stimulated ALP activity in a dose-dependent

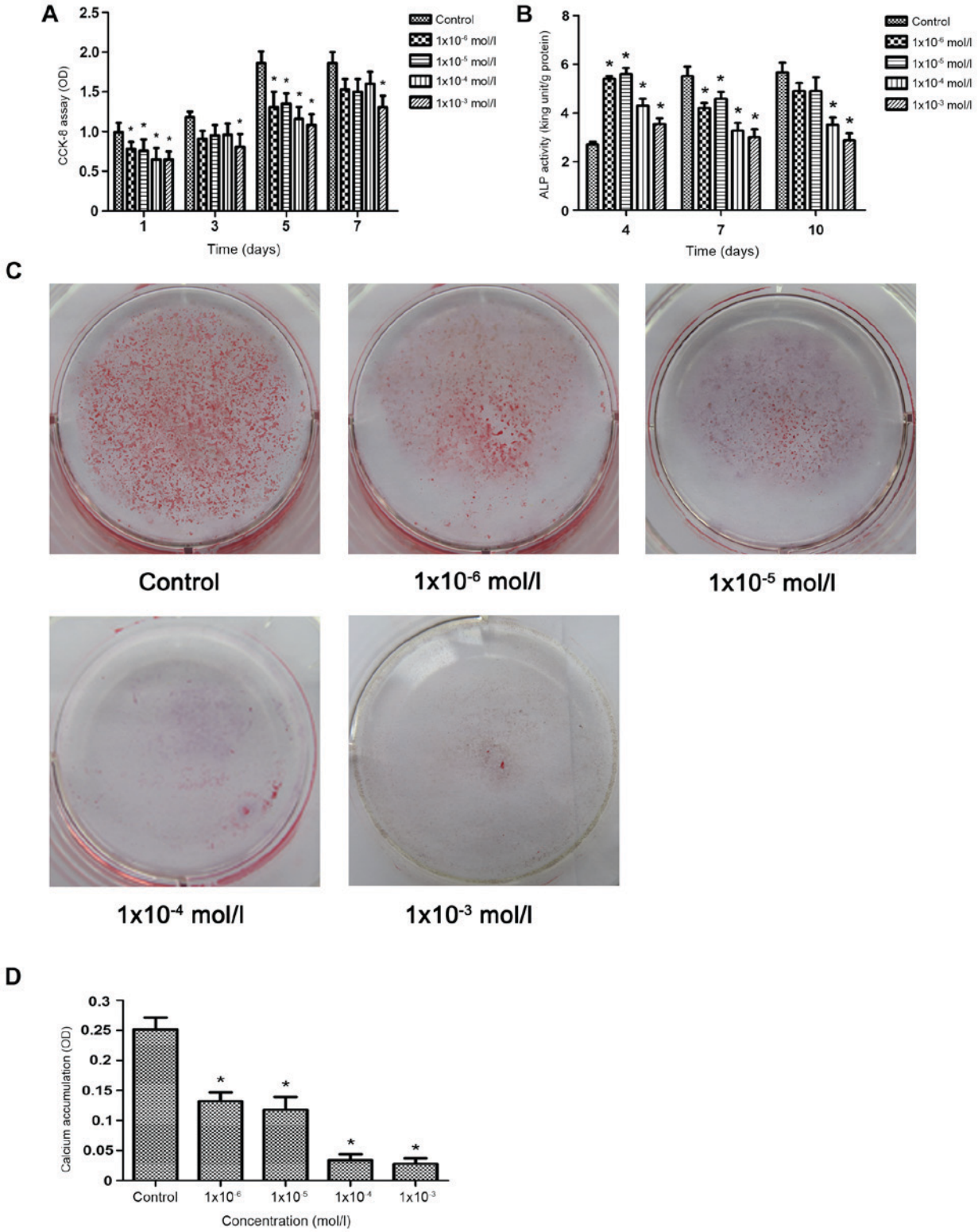

Figure 3. Effects of nicotine on cell proliferation, ALP activity and calcified nodule formation of Sprague-Dawley rat osteoblasts. (A) CCK-8 detection demonstrated that the proliferation of osteoblasts was significantly decreased in all nicotine groups at days 1 and 5, while proliferation was only inhibited at $1x10^{-3}$ mol/l nicotine at days 3 and 7, compared with the control group. (B) ALP activity in nicotine groups was significantly higher at day 4 compared with the control group, while ALP activity was reduced in nicotine-treated groups compared with the control group at days 7 and 10. (C) The alizarin red staining of the mineralized nodules was captured using a digital camera. (D) The formation of mineralized nodules decreased significantly at all nicotine concentrations after 21 days of culture compared with the control group. Each bar represents the mean ± standard deviation (n=) $^{*}P<0.05$ vs. control group. ALP, alkaline phosphatase; CCK-8, Cell Counting kit-8; OD, optical density.

fashion in UMR 106-01 rat osteoblastic osteosarcoma cells. Furthermore, nicotine was reported to inhibit the proliferation of osteoblasts as well as the expression of certain important osteogenic mediators in rabbit osteoblasts (23). Yuhara *et al* (11) further identified that in ROB-C26 cells, nicotine increased ALP activity in a dose-dependent manner and increased the

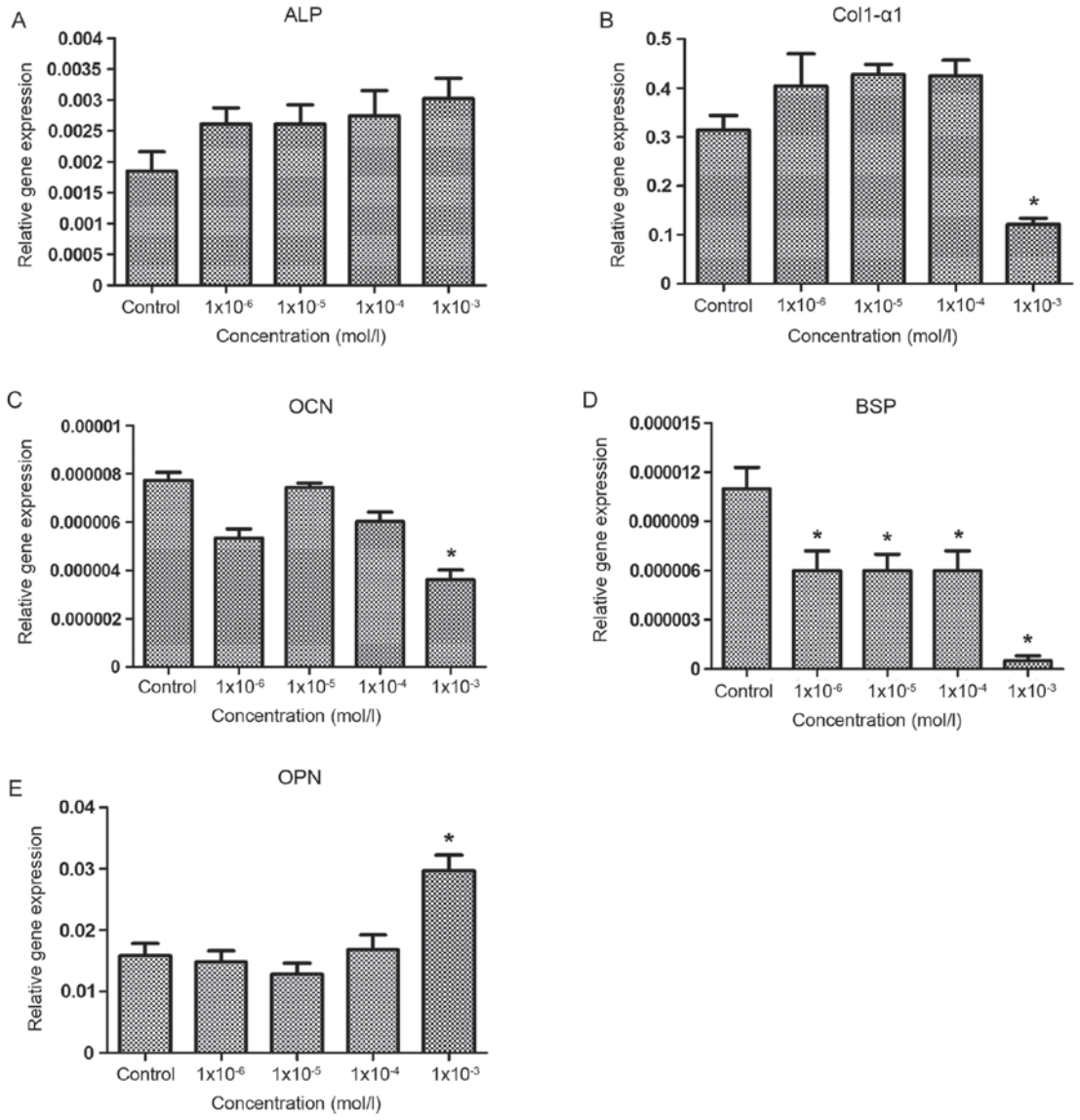

Figure 4. Effects of nicotine on the expression of Sprague-Dawley rat osteoblast metabolism-associated genes at day 7 of culture. (A) Nicotine exhibited no significant effects on the expression of ALP mRNA. The expression levels of (B) Col1-α1 and (C) OCN mRNA were significantly lower in the $1x10^{-3}$ mol/l nicotine group compared with the control group. (D) BSP mRNA expression was significantly lower in all nicotine groups compared with the control group. (E) OPN mRNA expression was significantly increased in the $1x10^{-3}$ mol/l nicotine group compared with the control group. Each bar represents the mean ± standard deviation (n=3) $^{*}P<0.05$ vs. control group. ALP, alkaline phosphatase; Col1-α1, collagen type I α1; OCN, osteocalcin; BSP, bone sialoprotein; OPN, osteopontin.

deposition of Ca^{2+} similarly. However, nicotine was reported to reduce these two activities in MC3T3-E1 cells. A previous study has also indicated that nicotine may affect bone metabolism in a biphasic manner, stimulating proliferation and gene expression at low doses analogous to concentrations acquired by light smokers, and suppressing proliferation at high doses analogous to concentrations acquired by heavy smokers (13). Although these studies used nicotine in similar concentrations to treat osteoblasts, the results differed from each other. These differences may have occurred as a result of differences in cell culture conditions, species differences, the type of osteoblast model selected, including differentiation stage, and differences in experimental designs. In previous studies, cell lines such as MC3T3-E1 and MG-63 were often used, whereas few studies have been performed on primary osteoblasts. After several passages of cell lines, apparent phenotypic heterogeneity can develop and cells may arrest at a certain stage of differentiation, therefore no longer fully reflecting the normal phenotype of osteoblasts (13,24). Compared with cell lines, primary osteoblast cells are more similar to human osteoblasts. In 1995, the U.S. Food and Drug Administration approved the use of the primary rat osteoblasts as osteoporosis and other bone metabolic disease models to evaluate preclinical and clinical drug efficacy (25). Consequently, in the present study, experiments were conducted on SD rat primary osteoblasts using nicotine at concentrations of $1x10^{-6}$, $1x10^{-5}$, $1x10^{-4}$ and $1x10^{-3}$ mol/l. These concentrations were selected based on nicotine levels of 0.06-1.2 mM/l detected in the blood of smokers of varying regularity; these concentrations were significantly lower compared with the 0.6-9.6 mM/l identified in the saliva (26).

In a previous study, 10^{-6} and 10^{-4} mol/l nicotine were reported to promote cell cycle progression during proliferation

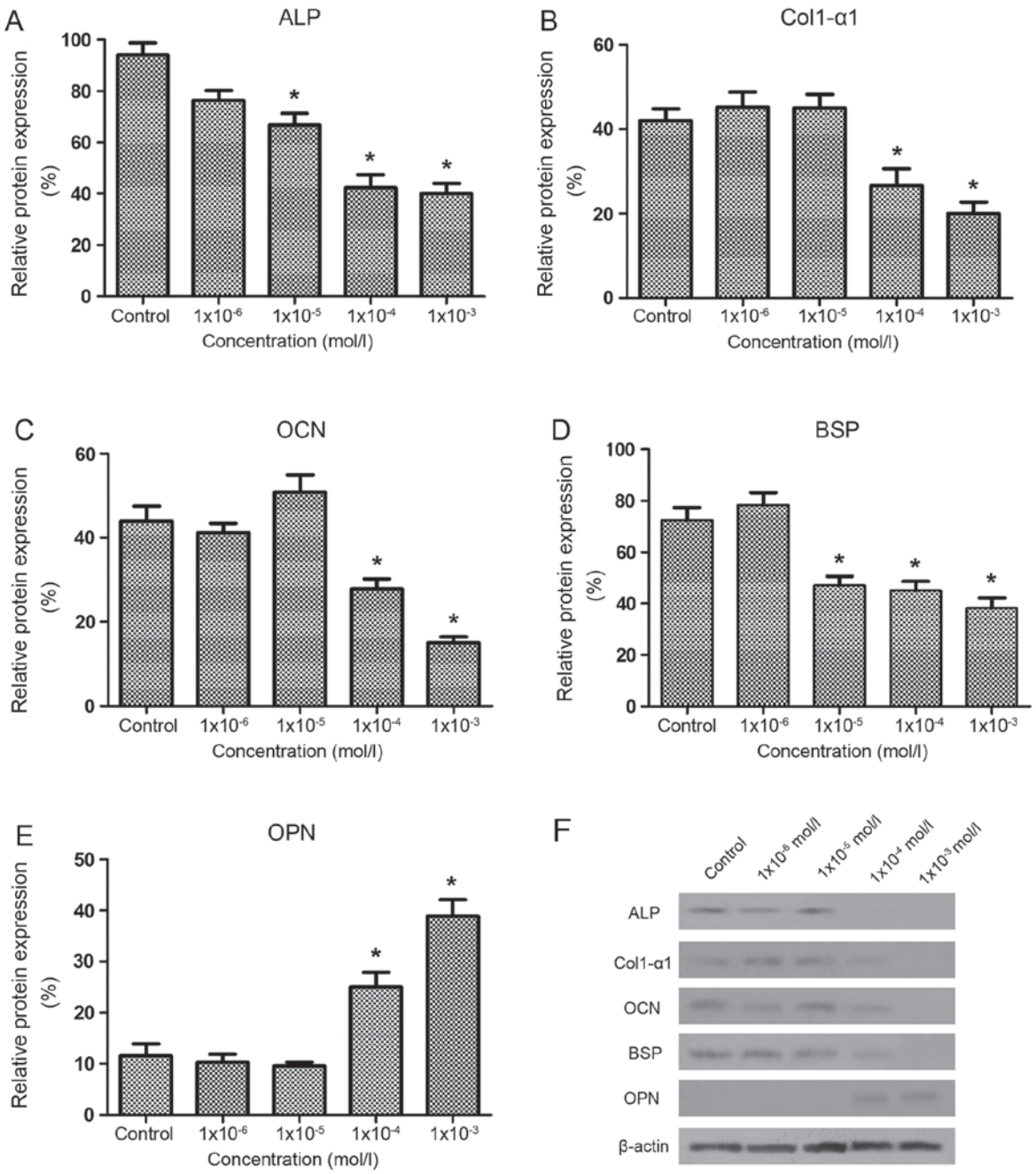

Figure 5. Effects of nicotine on the expression of Sprague-Dawley rat osteoblast metabolism-associated proteins at day 7 of culture. (A) Nicotine significantly decreased ALP protein expression in the $1x10^{-5}$, $1x10^{-4}$ and $1x10^{-3}$ mol/l nicotine groups compared with the control group. The protein levels of (B) Col1-α1 and (C) OCN were significantly decreased by nicotine in the $1x10^{-4}$ and $1x10^{-3}$ mol/l groups compared with the control group. (D) BSP proteins levels were significantly decreased by all concentrations of nicotine, excluding $1x10^{-6}$ mol/l, compared with the control group. (E) OPN protein was significantly increased by $1x10^{-3}$ and $1x10^{-4}$ mol/l nicotine compared with the control group. (F) Representative western blot bands for the protein expression of ALP, Col1-α1, OCN, BSP and OPN in Sprague-Dawley rat osteoblasts. Each bar represents the mean ± standard deviation (n=3) $^{*}P<0.05$ vs. control group. ALP, alkaline phosphatase; Col1-α1, collagen type I α1; OCN, osteocalcin; BSP, bone sialoprotein; OPN, osteopontin.

by downregulating p53 expression and upregulating cyclin D1 in the mouse pre-osteoblastic cell line MC3T3-E1 (27). However, the results of the present study revealed an inhibitory effect of nicotine on the proliferation of primary osteoblasts. The difference in the results may be due to the use of different cell models.

Apoptosis is an active programmed cell death process that, together with cell proliferation and differentiation, maintains the homeostasis of the organism (28). To the best of our knowledge, the effects of nicotine on osteoblast apoptosis have rarely been reported. In the present study, the early apoptosis of cells was significantly promoted by nicotine concentrations of 10^{-4} and 10^{-3} mol/l. However, the mechanism underlying this effect requires further investigation. Previous studies have demonstrated that members of the Bcl-2 family, including Bcl-2, Bcl-2-like 2 and Bcl-2-associated X, members of the caspase family, including caspase 1 and caspase 3, and the oncogene c-Myc may be involved in osteoblast apoptosis (29,30).

Table II. The top 10 upregulated genes that were differentially expressed in nicotine-treated osteoblasts compared with control cells.

Gene name	Fold change	P-value
Fgf21	6.212	0.0442
RGD1562667	6.067	0.0289
RGD1559482	6.057	0.0127
Fam25a	5.948	0.0021
Cd38	5.214	0.0035
Pla2g10	4.315	0.0074
Akr1c3	4.285	0.0043
Serpinb10	4.193	0.0005
Ccr1	4.125	0.0083
Ebi3	4.013	0.0011

Table III. The top 10 downregulated genes that were differentially expressed in nicotine-treated osteoblasts compared with control cells.

Gene name	Fold change	P-value
Notch1	5.466	0.0001
Hey2	4.727	0.0448
Ccdc40	4.000	0.0019
Cdhr4	3.893	0.0015
Adora2a	3.862	0.0001
Scin	3.754	0.0015
Smad3	3.715	0.0006
Slc25a47	3.646	0.0009
Sema3g	3.540	0.0205
Filip1	3.483	0.0001

Table IV. Osteogenesis-associated genes that were differentially expressed in nicotine-treated osteoblasts compared with control cells.

Gene name	Fold change	P-value	Regulation
Smad3	3.716	0.0007	Down
MMP-3	2.645	0.0001	Down
Ltbp2	2.11	0.0006	Down

Smad3, SMAD family member 3; MMP-3, matrix metallopeptidase 3; Ltbp2, latent transforming growth factor β-binding protein 2.

As an indicator of the differentiation potential of osteoblasts in the initial stage, ALP is able to hydrolyze the phosphate ester bonds on substrate molecules to generate phosphate ions, which have a strong affinity for Ca^{2+} (31). The quality and quantity of ALP is important in affecting the viability of osteoblasts. In previous studies, the effect of nicotine on the ALP activity of osteoblasts has been controversial. Yuhara *et al* (11) reported that nicotine reduced ALP activity in a dose-dependent manner in MC3T3-E1 cells and increased ALP activity in ROB-C26 cells during days 3-12. By contrast, Gullihorn *et al* (32) demonstrated that nicotine promoted ALP activity on day 3 in MC3T3-E1 cells. Sato *et al* (27) reported that following a transient increase in ALP activity at day 3, nicotine led to a marked reduction in the activity of ALP at day 7 in MC3T3-E1 cells, which is similar to the results of the present study. The results of the present study demonstrated that ALP activity was significantly higher in nicotine-treated groups compared with the control group at day 4, which may occur due to the stress response of the cells following nicotine stimulation and subsequent activation of the regulatory mechanism of ALP, potentially through the bone morphogenetic protein/Smads signaling pathway (33). In addition, studies have also demonstrated that nitric oxide affected the differentiation of osteoblast-like cells (34,35). Therefore, differences in the effects of nicotine on osteoblasts may be associated with differences in nitric oxide-associated pathways. Thus, it is noted that the regulatory effect of nicotine on the ALP activity of osteoblasts requires further confirmation and the regulatory mechanism, particularly the molecular pathways involved, also requires investigation.

During *in vitro* osteogenesis, Col1 functions as the scaffold for the nucleation of hydroxyapatite crystals and acts on osteoblast cells in an autocrine manner to promote the expression of ALP, OCN, OPN and osteonectin by activating the protein kinase C signal transduction pathway (36). OCN is usually expressed in the early stage of calcification and regulates the speed and direction of bone matrix mineral formation (37). OPN is a phosphorylated sialoprotein with a highly conserved RGD motif that interacts with various receptors, including αvβ3, αvβ1 and αvβ5, on the surface of some cell types, such as osteoclast and endothelial cells (38). A previous study has reported that the phosphorylation of OPN may inhibit the formation of hydroxyapatite crystals *in vitro* in a dose-dependent manner. The mechanism of this inhibition may involve OPN interacting with osteoclast surface integrins (primarily αvβ3) through the RGD motif to mediate osteoclast adhesion in bone tissue and promote bone resorption (39). OPN has also been reported to inhibit osteoblast differentiation (40). BSP is a highly sulfated and phosphorylated glycoprotein that nucleates hydroxyapatite crystal formation. Nakayama *et al* (41) identified that nicotine suppressed the transcription of BSP mediated through CRE, FRE and HOX elements within the proximal promoter of the BSP gene in rats. According to the results of the present study, it may be concluded that the inhibition of mineralized nodule formation may depend on the effect of nicotine on ALP activity at $1x10^{-6}$ mol/l, on the decrease of ALP and BSP protein at$1x10^{-5}$ mol/l and on the decrease of Col1-α1 and OCN protein, and the increase of OPN protein, at $1x10^{-4}$ and $1x10^{-3}$ mol/l nicotine. The inhibitory effect of nicotine on the expression levels of osteoblast metabolism associated mRNA and proteins was dose-dependent. Notably, in the presents study, the gene expression of each osteogenesis-associated factor was not completely consistent with the protein expression, which may be due to multiple regulatory steps that occur between transcription and translation.

The effects of nicotine on osteoblasts involve complex intracellular signal transduction pathways; however, the

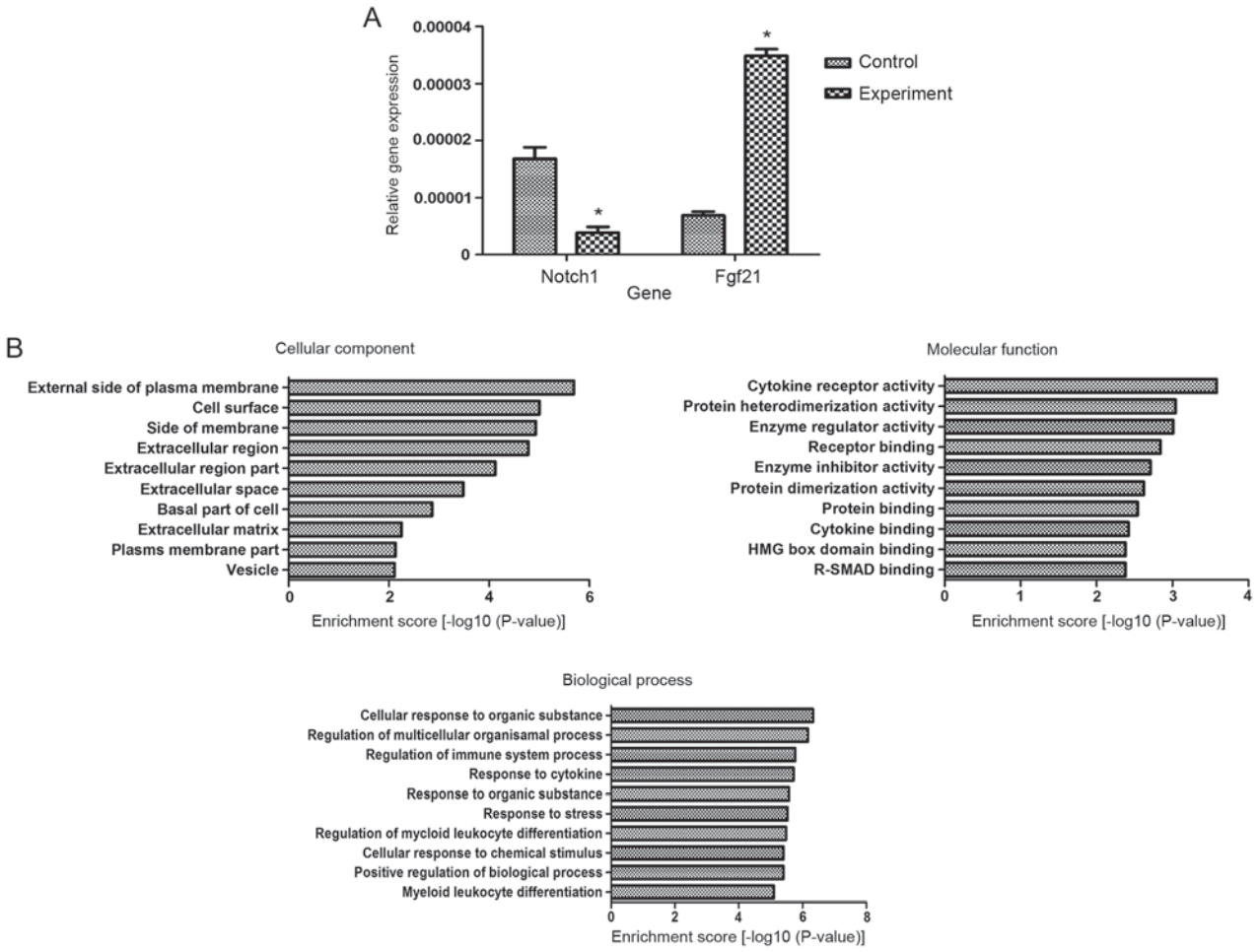

Figure 6. Effect of $1x10^{-3}$ mol/l nicotine on the whole genome expression profile of Sprague-Dawley rat osteoblasts. (A) Reverse transcription-quantitative polymerase chain reaction analyses of Fgf21 and Notch1 genes demonstrated that the expression of Notch1 was downregulated 5.67-fold and that Fgf21 expression was upregulated 5.94-fold in the osteoblasts of Sprague-Dawley rats treated with $1x10^{-3}$ mol/l nicotine compared with the control group, which was consistent with the microarray results. (B) Gene Ontology analysis indicated that $1x10^{-3}$ mol/l nicotine altered functions in cellular component, molecular function and biological process categories. Each bar represents the mean ± standard deviation (n=3) $^{*}P<0.05$ vs. control group. Fgf21, fibroblast growth factor 21.

specific molecular mechanism of regulation remains to be elucidated. The whole genome expression microarray is a high-throughput gene detection method that can provide a reliable basis for investigating the molecular regulatory mechanism of biological effects by utilizing bioinformatics analysis to evaluate the expression of genes in cells rapidly and comprehensively. GO analysis indicated that nicotine altered several functions of the SD rat osteoblasts, including organic metabolism, intercellular biological process regulation, cytokine receptor activity, inflammatory response, ion transport, calcium ion adhesion and transcription factor adhesion. KEGG pathway analysis demonstrated that these differentially expressed genes were primarily involved in pathways concerning proliferation, differentiation, apoptosis, adhesion and carcinogenesis. Among the pathways identified, the Hedgehog and Notch pathways have been reported to directly regulate osteoblast differentiation (42,43).

In the Hedgehog pathway, Sonic hedgehog protein acts as an important signal molecule in the early stage of osteoblast differentiation, while Indian hedgehog protein (Ihh) is involved in the later stage to promote the differentiation and maturation of osteoblasts (44). The results of the present study demonstrated that the expression of Ihh was significantly decreased following nicotine treatment, indicating that nicotine may inhibit the proliferation, differentiation and function of SD rat osteoblasts by disturbing the Hedgehog signaling pathway.

Concerning the role of the Notch pathway in the regulation of osteoblast differentiation, *in vitro* studies have reported contrasting results. Certain studies demonstrated that the overexpression of Notch1, one of the notch receptors, inhibited osteoblastic differentiation (45,46). Conversely, Tezuka *et al* (47) demonstrated that osteoblastic cell differentiation was regulated positively by Notch1. In the present study, the results demonstrated that the expression of Notch1 was significantly decreased following nicotine treatment, indicating that nicotine may inhibit the activation of the Notch signaling pathway and thereby decrease osteoblastic proliferation. However, this hypothesis requires confirmation.

In conclusion, the present study demonstrated that nicotine exhibited an inhibitory effect on SD rat osteoblast metabolism. Microarray analysis revealed that the Notch and Hedgehog signaling pathways were enriched with differentially expressed genes in osteoblasts following nicotine treatment and that these pathways were strongly associated with osteoblast differentiation, which may result in improved future understanding of nicotine-induced bone diseases. These results may

Table V. Kyoto Encyclopedia of Genes and Genomes pathway analysis of the top 10 significantly upregulated genes following nicotine treatment.

Pathway ID	Definition	Count	P-value	Genes
rno04640	Hematopoietic cell lineage (rat)	4	0.0005	CD34, CD38, IL2RA, ITGA2
rno04921	Oxytocin signaling pathway (rat)	5	0.0008	CCND1, CD38, FOS, JUN, MYLK3
rno04510	Focal adhesion (rat)	5	0.0028	ACTN3, CCND1, ITGA2, JUN, MYLK3
rno04380	Osteoclast differentiation (rat)	4	0.0029	FCGR2B, FOS, JUN, LILRA5
rno05210	Colorectal cancer (rat)	3	0.0033	CCND1, FOS, JUN
rno04630	Jak-STAT signaling pathway (rat)	4	0.0044	BCL2L1, CCND1, IL2RA, TSLP
rno04662	B cell receptor signaling pathway (rat)	3	0.0046	FCGR2B, FOS, JUN
rno05133	Pertussis (rat)	3	0.0046	C1QC, FOS, JUN
rno05412	Arrhythmogenic right ventricular cardiomyopathy (ARVC) (rat)	3	0.0050	ACTN3, ITGA2, SGCG
rno05222	Small cell lung cancer (rat)	3	0.0080	BCL2L1, CCND1, ITGA2

Table VI. Kyoto Encyclopedia of Genes and Genomes pathway analysis of the top 10 significantly downregulated genes following nicotine treatment.

Pathway ID	Definition	Count	P-value	Genes
rno05150	*Staphylococcus aureus* infection (rat)	4	0.0002	C3, C4A, CFB, SELP
rno05133	Pertussis (rat)	4	0.0007	C3, C4A, C4BPA, IL23A
rno04610	Complement and coagulation cascades (rat)	4	0.0007	C3, C4A, C4BPA, CFB
rno05322	Systemic lupus erythematosus (rat)	4	0.0058	C3, C4A, HIST1H2AN, HIST1H3A
rno05323	Rheumatoid arthritis (rat)	3	0.0128	IL23A, MMP3, TNFSF11
rno04514	CAMs (rat)	4	0.0156	CLDN4, NEGR1, NTNG1, SELP
rno05033	Nicotine addiction (rat)	2	0.0212	CACNA1B, GABRA1
rno04668	TNF signaling pathway (rat)	3	0.0227	BIRC3, CX3CL1, MMP3
rno04340	Hedgehog signaling pathway (rat)	2	0.0298	IHH, LRP2
rno04330	Notch signaling pathway (rat)	2	0.0345	DLL3, NOTCH1

Table VII. Differentially expressed genes associated with Hedgehog and Notch signaling pathways following nicotine treatment.

Gene name	Fold change	P-value	Regulation	Pathway
IHH	2.619	0.0016	Down	Hedgehog
LRP2	2.406	0.0058	Down	Hedgehog
DLL3	2.056	0.0087	Up	Notch
NOTCH1	5.466	0.0001	Down	Notch

IHH, Indian hedgehog; LRP2, low density lipoprotein receptor-related protein 2; DLL3, delta-like 3.

provide a theoretical basis for the prevention and treatment of smoking-related diseases in the future.

Acknowledgements

Not applicable.

Funding

The present study was supported by the Sichuan science and technology support project, Chengdu, China (grant no. 2014SZ0019).

Availability of data and materials

The datasets used and analyzed during the current study are available from the corresponding author on reasonable request.

Authors' contributions

HW conceived and designed the present study. DL and KW performed cell culture, western blot analyses, reverse transcription-quantitative polymerase chain reaction and microarray analysis, and were also the predominant contributors in the writing of the manuscript. ZT and RL performed experiments for the determination of cellular proliferation, apoptosis, alkaline phosphatase activity and formation of mineralized nodules. FZ and MC analyzed and interpreted the data. QL made contributions to interpretation of data and

critically revised the manuscript for important intellectual content. All authors read and approved the final manuscript.

Ethics approval and consent to participate

The current study was approved by the Ethics Committee of West China Hospital of Stomatology of Sichuan University (Chengdu, China).

Consent for publication

Not applicable.

Competing interests

The authors declare that they have no competing interests.

References

1. Vellappally S, Fiala Z, Smejkalová J, Jacob V and Somanathan R: Smoking related systemic and oral diseases. Acta Medica (Hradec Kralove) 50: 161-166, 2007.
2. Johnson GK and Guthmiller JM: The impact of cigarette smoking on periodontal disease and treatment. Periodontol 44: 178-194, 2007.
3. Tymkiw KD, Thunell DH, Johnson GK, Joly S, Burnell KK, Cavanaugh JE, Brogden KA and Guthmiller JM: Influence of smoking on gingival crevicular fluid cytokines in severe chronic periodontitis. J Clin Periodontol 38: 219-228, 2011.
4. Heitz-Mayfield LJ and Huynh-Ba G: History of treated periodontitis and smoking as risks for implant therapy. Int J Oral Maxillofac Implants 24 (Suppl): S39-S68, 2009.
5. Larrazábal C, García B, Peñarrocha M and Peñarrocha M: Influence of oral hygiene and smoking on pain and swelling after surgical extraction of impacted mandibular third molars. J Oral Maxillofac Surg 68: 43-46, 2010.
6. García B, Penarrocha M, Martí E, Gay-Escodad C and Von Arx T: Pain and swelling after periapical surgery related to oral hygiene and smoking. Oral Surg Oral Med Oral Pathol Oral Radiol Endod 104: 271-276, 2007.
7. Krall EA, Abreu Sosa C, Garcia C, Nunn ME, Caplan DJ and Garcia RI: Cigarette smoking increases the risk of root canal treatment. J Dent Res 85: 313-317, 2006.
8. Henningfield JE and Goldberg SR: Progress in understanding the relationship between the pharmacological effects of nicotine and human tobacco dependence. Pharmacol Biochem Behav 30: 217-220, 1988.
9. En-Nosse M, Hartmann S, Trinkaus K, Alt V, Stigler B, Heiss C, Kilian O, Schnettler R and Lips KS: Expression of non-neuronal cholinergic system in osteoblast-like cells and its involvement in osteogenesis. Cell Tissue Res 338: 203-215, 2009.
10. Alford AI and Hankenson KD: Matricellular proteins: Extracellular modulators of bone development, remodeling, and regeneration. Bone 38: 749-757, 2006.
11. Yuhara S, Kasagi S, Inoue A, Otsuka E, Hirose S and Hagiwara H: Effects of nicotine on cultured cells suggest that it can influence the formation and resorption of bone. Eur J Pharmacol 383: 387-393, 1999.
12. Ramp WK, Lenz LG and Galvin RJ: Nicotine inhibits collagen synthesis and alkaline phosphatase activity, but stimulates DNA synthesis in osteoblast-like cells. Proc Soc Exp Biol Med 197: 36-43, 1991.
13. Rothem DE, Rothem L, Soudry M, Dahan A and Eliakim R: Nicotine modulates bone metabolism-associated gene expression in osteoblast cells. J Bone Miner Metab 27: 555-561, 2009.
14. Rothem DE, Rothem L, Dahan A, Eliakim R and Soudry M: Nicotinic modulation of gene expression in osteoblast cells, MG-63. Bone 48: 903-909, 2011.
15. Torshabi M, Esfahrood ZR, Gholamin P and Karami E: Effects of nicotine in the presence and absence of vitamin E on morphology, viability and osteogenic gene expression in MG-63 osteoblast-like cells. J Basic Clin Physiol Pharmacol 27: 595-602, 2016.
16. Livak KJ and Schmittgen TD: Analysis of relative gene expression data using real-time quantitative PCR and the 2(-Delta Delta C(T)) method. Methods 25: 402-408, 2001.
17. Harris MA, Clark J, Ireland A, Lomax J, Ashburner M, Foulger R, Eilbeck K, Lewis S, Marshall B, Mungall C, *et al*: The Gene Ontology (GO) database and informatics resource. Nucleic Acids Res 32 (Database Issue): D258-D261, 2004.
18. Ogata H, Goto S, Sato K, Fujibuchi W, Bono H and Kanehisa M: KEGG: Kyoto encyclopedia of genes and genomes. Nucleic Acids Res 27: 29-34, 1999.
19. Zanotti S, Smerdel-Ramoya A, Stadmeyer L, Durant D, Radtke F and Canalis E: Notch inhibits osteoblast differentiation and causes osteopenia. Endocrinology 149: 3890-3899, 2008.
20. Canalis E: Role of Notch signaling in osteoblast differentiation and bone remodeling. Bone 45 (Suppl 3): S120-S121, 2009.
21. Shi Y, Chen J, Karner CM and Long F: Hedgehog signaling activates a positive feedback mechanism involving insulin-like growth factors to induce osteoblast differentiation. Proc Natl Acad Sci USA 112: 4678-4683, 2015.
22. Fang MA, Frost PJ, Iida-Klein A and Hahn TJ: Effects of nicotine on cellular function in UMR 106-01 osteoblast-like cells. Bone 12: 283-286, 1991.
23. Ma L, Zwahlen RA, Zheng LW and Sham MH: Influence of nicotine on the biological activity of rabbit osteoblasts. Clin Oral Implants Res 22: 338-342, 2011.
24. Wang D, Christensen K, Chawla K, Xiao G, Krebsbach PH and Franceschi RT: Isolation and characterization of MC3T3-E1 preosteoblast subclones with distinct in vitro and in vivo differentiation/mineralization potential. J Bone Miner Res 14: 893-903, 1999.
25. Thompson DD, Simmons HA, Pirie CM and Ke HZ: FDA Guidelines and animal models for osteoporosis. Bone 17 (4 Suppl): 125S-133S, 1995.
26. Benowitz NL: Drug therapy. Pharmacologic aspects of cigarette smoking and nicotine addition. N Engl J Med 319: 1318-1330, 1988.
27. Sato T, Abe T, Nakamoto N, Tomaru Y, Koshikiya N, Nojima J, Kokabu S, Sakata Y, Kobayashi A and Yoda T: Nicotine induces cell proliferation in association with cyclin D1 up-regulation and inhibits cell differentiation in association with p53 regulation in a murine pre-osteoblastic cell line. Biochem Biophys Res Commun 377: 126-130, 2008.
28. Peter ME: Programmed cell death: Apoptosis meets necrosis. Nature 471: 310 312, 2011.
29. Youle RJ and Strasser A: The BCL-2 protein family: Opposing activities that mediate cell death. Nat Rev Mol Cell Biol 9: 47-59, 2008.
30. Ola MS, Nawaz M and Ahsan H: Role of Bcl-2 family proteins and caspases in the regulation of apoptosis. Mol Cell Biochem 351: 41-58, 2011.
31. Golub EE, Harrison G, Taylor AG, Camper S and Shapiro IM: The role of alkaline phosphatase in cartilage mineralization. Bone Miner 17: 273-278, 1992.
32. Gullihorn L, Karpman R and Lippiello L: Differential effects of nicotine and smoke condensate on bone cell metabolic activity. J Orthop Trauma 19: 17-22, 2005.
33. Kuo PL, Hsu YL, Chang CH and Chang JK: Osthole-mediated cell differentiation through bone morphogenetic protein-2/p38 and extracellular signal-regulated kinase 1/2 pathway in human osteoblast cells. J Pharmacol Exp Ther 314: 1290-1299, 2005.
34. Koyama A, Otsuka E, Inoue A, Hirose S and Hagiwara H: Nitric oxide accelerates the ascorbic acid-induced osteoblastic differentiation of mouse stromal ST2 cells by stimulating the production of prostaglandin E(2). Eur J Pharmacol 391: 225-231, 2000.
35. MacPherson H, Noble BS and Ralston SH: Expression and functional role of nitric oxide synthase isoforms in human osteoblast-like cells. Bone 24: 179-185, 1999.
36. Green J, Schotland S, Stauber DJ, Kleeman CR and Clemens TL: Cell-matrix interaction in bone: Type I collagen modulates signal transduction in osteoblast-like cells. Am J Physiol 268: 1090-1103, 1995.
37. Boskey AL, Gadaleta S, Gundberg C, Doty SB, Ducy P and Karsenty G: Fourier transform infrared microspectroscopic analysis of bones of osteocalcin-deficient mice provides insight into the function of osteocalcin. Bone 23: 187-196, 1998.
38. Giachelli CM, Schwartz SM and Liaw L: Molecular and cellular biology of osteopontin Potential role in cardiovascular disease. Trends Cardiovasc Med 5: 88-95, 1995.

39. Chellaiah MA, Kizer N, Biswas R, Alvarez U, Strauss-Schoenberger J, Rifas L, Rittling SR, Denhardt DT and Hruska KA: Osteopontin deficiency produces osteoclast dysfunction due to reduced CD44 surface expression. Mol Biol Cell 14: 173-189, 2003.
40. Kojima H, Uede T and Uemura T: In vitro and in vivo effects of the overexpression of osteopontin on osteoblast differentiation using a recombinant adenoviral vector. J Biochem 136: 377-386, 2004.
41. Nakayama Y, Mezawa M, Araki S, Sasaki Y, Wang S, Han J, Li X, Takai H and Ogata Y: Nicotine suppresses bone sialoprotein gene expression. J Periodontal Res 44: 657-663, 2009.
42. Zanotti S and Canalis E: Notch and the skeleton. Mol Cell Biol 30: 886-896, 2010.
43. Day TF and Yang Y: Wnt and hedgehog signaling pathways in bone development. J Bone Joint Surg Am 90 (Suppl 1): S19-S24, 2008.
44. Tu X, Joeng KS and Long F: Indian hedgehog requires additional effectors besides Runx2 to induce osteoblast differentiation. Dev Biol 362: 76-82, 2012.
45. Deregowski V, Gazzerro E, Priest L, Rydziel S and Canalis E: Notch 1 overexpression inhibits osteoblastogenesis by suppressing Wnt/beta-catenin but not bone morphogenetic protein signaling. J Biol Chem 281: 6203-6210, 2006.
46. Sciaudone M, Gazzerro E, Priest L, Delany AM and Canalis E: Notch 1 impairs osteoblastic cell differentiation. Endocrinology 144: 5631-5639, 2003.
47. Tezuka K, Yasuda M, Watanabe N, Morimura N, Kuroda K, Miyatani S and Hozumi N: Stimulation of osteoblastic cell differentiation by notch. J Bone Miner Res 17: 231-239, 2002.